coatings

MDPI

Article

Target Voltage Hysteresis Behavior and Control Point in the Preparation of Aluminum Oxide Thin Films by Medium Frequency Reactive Magnetron Sputtering

Qingfu Wang *,†, Liping Fang *,†, Qinghe Liu, Lin Chen, Qinguo Wang, Xiandong Meng and Hong Xiao

Institute of Materials, China Academy of Engineering Physics, Mianyang 621700, China; lqhsylz@sina.com (Q.L.); sva.chlin@163.com (L.C.); sevenstarchong@sina.com (Q.W.); mengxiandong@caep.cn (X.M.); xiaohongcaep@163.com (H.X.)

* Correspondence: wqf415108@sina.cn (Q.W.); fanglp26@163.com (L.F.)

† These authors contribute equally to this work.

Received: 16 March 2018; Accepted: 16 April 2018; Published: 18 April 2018

Abstract: Aluminum oxide thin films were prepared by medium frequency reactive magnetron sputtering. The target voltage hysteresis behavior under different argon partial pressure and target power conditions were studied. The results indicate that the target voltage hysteresis loop of aluminum oxide thin film preparation has typical behavior of that for reactive sputtering deposition of compound films. The target voltage feedback control approach was applied to circumvent the hysteresis problem. The microstructure and chemical composition of the aluminum oxide thin films prepared at different target voltage control points were investigated by X-ray diffraction, scanning electron microscopy, energy dispersive X-ray spectroscopy and Auger electron spectroscopy. The results indicated that the prepared aluminum oxide thin films, which are compact and mostly amorphous, can be obtained with target voltage control point in the range of 25~35%.

Keywords: aluminum oxide; thin film; medium frequency; magnetron sputtering; target voltage; hysteresis loop

1. Introduction

Aluminum oxide is a widely used functional thin film in the fields of optics, microelectronics and mechanisms, due to its excellent chemical stability, mechanical strength, high hardness, anti-corrosion and anti-wear properties and optical properties [1–5]. As a surface protective coating for highly active metals, aluminum oxide film bears substantial potential to enhance the wear and corrosion resistance of metal surfaces by forming multilayered aluminum/aluminum oxide coatings, with the possible merits of higher density, better adhesion properties, and lower residual stress than the two single layer coatings alone [1,2,6,7]. In this work we report our investigations on the preparation of aluminum oxide thin films deposited by reactive magnetron sputtering, which is a common technique in the preparation of compound thin films and coatings.

Reactive magnetron sputtering is realized in magnetron sputtering with a reactive gas (such as oxygen or nitrogen) introduced into the vacuum chamber, in addition to an inert working gas [8–12]. There are several reactive magnetron sputtering techniques, i.e., direct current reactive magnetron sputtering (DCRMS) [10], pulsed reactive magnetron sputtering (PMS) [11], radio frequency reactive magnetron sputtering (RFRMS) [12] and medium frequency reactive magnetron sputtering (MFRMS) [9], which are ordered according to the frequency of the power supply of the sputtering target. The disadvantages of DCRMS are target poisoning and arc problems, and the prepared films

often have large embedded particles, which renders the deposition processes hard to control and reproduce [13]; the demerits of RFRMS are the high-cost of equipment and low deposition rates [14]; thus neither of these two techniques is suitable for the preparation of high quality thin films and coatings at an industrial level. High power impulse magnetron sputtering (HiPIMS) is an emerging reactive magnetron sputtering technique, which could produce high density films [15–17]. However, this technique still has several aspects which need to be improved: the high cost of the power supply, the instability of the plasma, low deposition rate, and self-sputtering, etc.

MFRMS uses a twin sputtering targets, which alternatively act as the anode and cathode. It is therefore able to effectively circumvent arc discharge and bypass the phenomenon of the disappearing anode [18]. Thus, stable deposition processes could be achieved with high reproducibility and high deposition rate. In this work, MFRMS is utilized to prepare aluminum oxide films to ensure the stability and reproducibility.

There are several parameters that could affect the processes of reactive magnetron sputtering, such as argon partial pressure, target power, target voltage, etc. Although the argon partial pressure and the target power could be easily controlled, the surface condition of the sputtering target varies in sputtering processes. Furthermore, we have noticed that under identical argon partial pressure and target power conditions, the target voltage falls as the thickness of the sputtering target decreases; this is possibly due to the enhanced magnetic field strength near the target surface [19].

During reactive magnetron sputtering, the target voltage changes as the variation of the flow rate of the reactive gas. The variation curves of the target voltage do not overlap between gradually increasing and decreasing the flow rate of the reactive gas, i.e., target voltage hysteresis behavior exists [18]. Three sputtering modes exist under different target voltages, i.e., the metallic mode, the mixed (or transition) mode, and the compound mode. The structure and composition of the films obtained under these three modes are quite different. In order to obtain thin films with high deposition rates and optimum properties, several approaches have been proposed to circumvent the hysteresis problem, such as: increasing the pumping speed [20], using the optical emission spectroscopic signal from the sputtered material, using the target voltage or direct mass spectrometry measurements as the feedback signals to directly control the partial pressure of the reactive gas during reactive sputtering deposition [18], etc. Among these approaches, the target voltage control seems probably to be the most effective approach, since the flow rate of the reactive gas could be stabilized at a desired level via the feedback control of the target voltage.

Many studies exist for the hysteresis behavior of the target voltage, but most of them use manual control of the reactive gas flow (see [21] and references therein). Therefore, not enough data points could be obtained, and the effective voltage control points are not optimized. The obtained thin films therefore show significant fluctuations of the film structure and chemical composition. In this work, a closed-loop feedback controller is used in the reactive sputtering deposition processes of aluminum oxide, which could measure the voltage hysteresis loops with high accuracy. Based on these hysteresis loops, as well as the structure and composition properties of the obtained aluminum oxide films, the optimal range of the target voltage control point was obtained.

2. Materials and Methods

2.1. Sample Preparation

A home-made magnetron sputtering system equipped with two circular planar Al (99.99% purity) sputtering targets was used to prepare the aluminum oxide films on Si (111) substrates. The two sputtering targets were powered by a 40 kHz medium frequency power source (Advanced Energy PEII, Fort Collins, CO, USA). The vacuum chamber was made of 304 stainless steel and sealed by fluororubber. The chamber was evacuated by two turbomolecular pumps backed by a roots blower and a mechanical pump. The setup of the deposition system is shown in Figure 1. The Si substrates were cleaned with 1% hydrofluoric acid solution for 5 min to remove surface oxides, and then rinsed

in de-ionized water and ethanol in an ultrasonic bath for 10 min each. Before deposition, the Al targets were pre-sputtered for 15 min to remove the surface oxide and contaminations. The base pressure of the sputtering chamber is lower than 5.0×10^{-4} Pa, and the working gases are argon (99.99% purity) and oxygen (99.99% purity). The partial pressure of argon was maintained at 0.3 Pa during all the film deposition processes, unless otherwise indicated. The flow of oxygen was controlled via a reactive sputtering controller (Speedflo mini, Gencoa Ltd., Liverpool, UK), equipped with a digital mass flow controller (EL-FLOW, Bronkhorst High-Tech B.V., Ruurlo, The Netherlands). The sputtering target was fixed at 1.0~1.5 kW and the target-substrate distance was kept at 180 mm. The deposition time for all of the samples was 60 min.

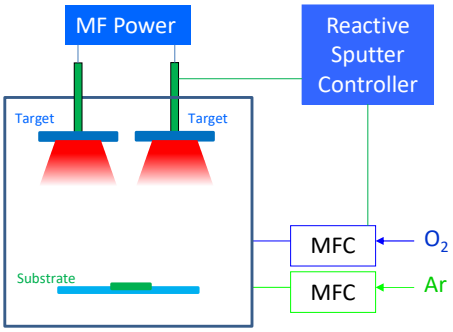

Figure 1. Schematic of the MFRMS system for aluminum oxide film preparation.

2.2. Target Voltage Hysteresis Loop Measurements

The flow of oxygen in reactive sputtering was controlled by the reactive sputtering controller. For target voltage hysteresis loop measurements, the flow curve of oxygen was set to follow the pattern shown in Figure 2. The flow rate of oxygen first increased, from 0 to 50 sccm (standard cubic centimeters per minute) at the rate of 25 sccm/min, and then decreased, to 0 sccm at similar rate. The target voltage was recorded automatically as the variation of the oxygen flow rate.

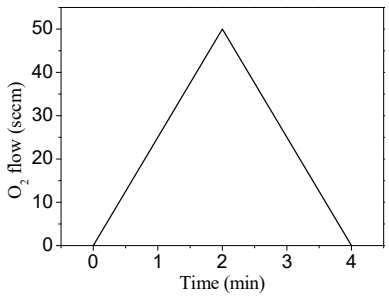

Figure 2. Flow curve of oxygen during target voltage hysteresis loop measurements.

2.3. Film Characterization

The structure of the prepared aluminum oxide films were characterized by grazing incidence X-ray diffraction (XRD, Phillips X'Pert Pro, New York City, NY, USA) with Cu Kα radiation and incident angle of 2° in the θ–2θ mode. The surface morphology and chemical composition were characterized by a field-emission scanning electron microscope (FESEM, FEI Helios Nanofab 600i, Lausanne, Switzerland) equipped with an energy dispersive X-ray spectroscope (EDS, Bruker QUANTAX 100, Berlin, Germany). The surface chemical composition was characterized by scanning Auger electron spectrometry (AES, Physical Electronics PHI-650, Chanhassen, MN, USA). The film thickness was measured by a stylus profiler (KLA-Tencor P-7, Milpitas, CA, USA).

3. Results

3.1. Target Voltage Hysteresis Loop

During the reactive sputtering deposition process, the variation of target voltage according to changes in the oxygen flow rate demonstrates hysteresis behavior; a typical hysteresis loop is shown in Figure 3 [21]. When the reactive gas starts to be added to the vacuum chamber, the metallic atoms sputtered away from the target, consuming the added reactive gas molecules; a compound is therefore not formed on the target surface. At this stage, the sputtering mode is metallic and an increase in level of the reactive gas yields little change in the target voltage. The ejected species are metallic at this stage.

When the flow of the reactive gas reaches a critical rate, the compound starts to partially cover the sputtering target, and the target voltage decreases significantly. At this stage, the sputtering mode is the mixed mode of metal and compound, and the ejected species are in the form of a mixture of metal and compound.

Further increasing the flow rate of reactive gas, compound films would fully cover the sputtering target. At this stage, sputtering is in compound mode, and further increasing the reactive gas flow yields little variation on the target voltage. The ejected species are compounds at this stage.

However, when gradually decreasing the reactive gas flow rate, the target voltage variation curve will not follow the curve while increasing the gas flow, i.e., hysteresis behavior, as shown in Figure 3, exists for the target voltage [18]. The target voltage significantly increases only when the reactive gas flow rate drops significantly. The sputtering mode changes from compound to the mixed mode, and finally goes back to the metallic mode with a decrease in the reactive gas flow.

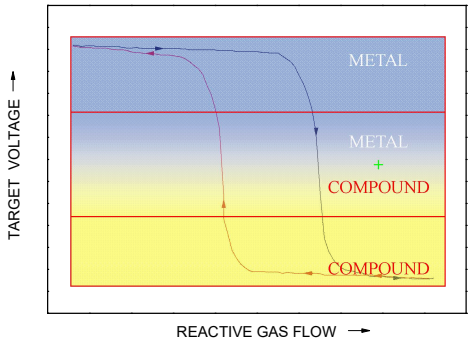

Figure 3. A typical target voltage hysteresis loop.

The hysteresis behavior of target voltage has direct connection with the sputtering power and argon partial pressure [22]. The hysteresis loops under different sputtering power (1.0~1.5 kW) and argon partial pressure (0.2~0.5 Pa) were measured and the results are shown in Figure 4.

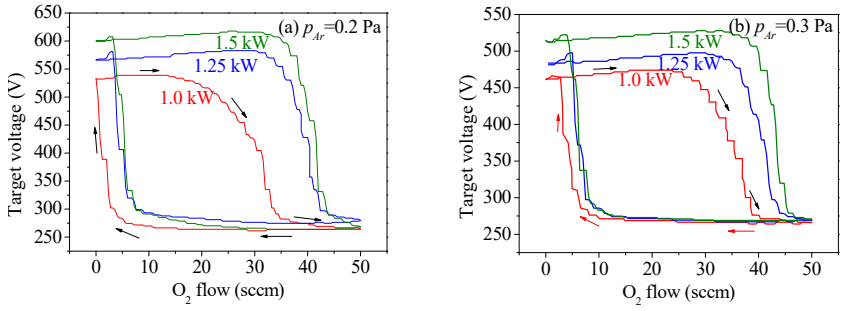

Figure 4. *Cont.*

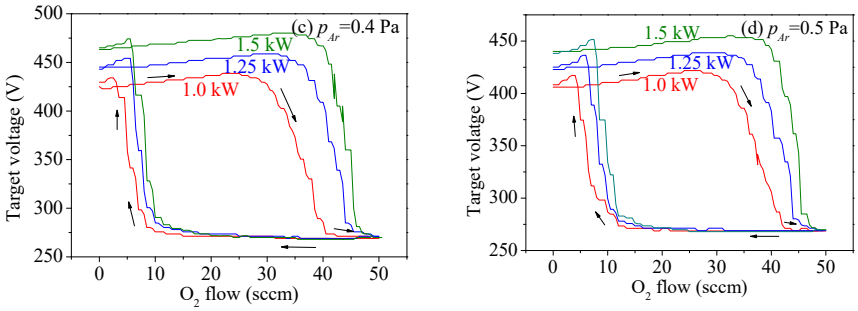

Figure 4. Target voltage hysteresis loops at different argon partial pressure and target power.

The results shown in Figure 4 have similar features as the typical hysteresis loop shown in Figure 3. It is illustrated in Figure 4a that under the argon partial pressure of 0.2 Pa, the target voltage increases from approximately 530 V to 600 V as the sputtering power rises from 1.0 kW to 1.5 kW. When the oxygen flow increases above 30 sccm, the target voltage starts to drop substantially with an increase in oxygen flow. This is mainly due to oxide formation on the target surface. Because the secondary electron emission coefficient of aluminum oxide is larger than that of metallic aluminum (see, for example, [23]), the formation of oxide enhances electron density in the glow discharge plasma near the target surface. The collision probabilities of electrons with argon atoms increases; therefore, the resistance of the plasma near the target surface drops, finally leading to a significant decrease in the target voltage. The target voltage becomes stable when the oxygen flow reaches 45 sccm. At this stage, the sputtering target is in the mode with overflow of oxygen, the target surface is fully covered by oxide, and sputtering is then in the compound mode.

As the oxygen flow gradually decreases from 50 sccm, the target voltage remains almost stable until 10 sccm, at which point the target voltage starts to soar with a further decrease in the oxygen flow. Similar hysteresis behaviors have been observed when the argon partial pressure was fixed at 0.3, 0.4 and 0.5 Pa, respectively.

Based on the results shown in Figure 4, the influence of argon partial pressure on the hysteresis loops at similar sputtering power of 1.5 kW is plotted in Figure 5. It is depicted that the target voltage for the metallic mode increases with a decrease in the argon partial pressure. This is mainly due to the reduction of the amount, and the resultant collision probability, of argon ions in the glow discharging plasma, thereby enhancing the sputtering strength of the oxide on the target surface. Low levels of oxide coverage of the sputtering target favor an increase in the target voltage.

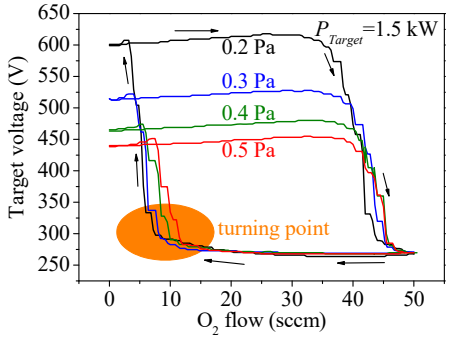

Figure 5. Influence of argon partial pressure on the target voltage hysteresis loop.

In the state of overflow of oxygen, the target surface is fully covered by oxide. At lower argon partial pressure, less argon ions take part in sputtering the oxide away. Therefore, a longer time is needed for the target surface to move back to the metallic mode. This is evidenced by the fact that the

oxygen flow, at the lower turning point of the compound mode to the metallic mode, decreases with the drop in the argon partial pressure, as highlighted in Figure 5.

The result illustrated in Figure 5 also indicates that under fixed target power, the argon partial pressure has little influence on the characteristics of the hysteresis curve between the compound mode and the metallic mode when decreasing the flow rate of oxygen. Note that the target voltages at this state are all roughly the same, i.e., approximately 260 V, regardless of the argon partial pressure. One can conclude that under these experimental conditions, the target voltage is hardly affected by the reactive gas pressure and the plasma composition. A similar phenomenon has been observed by Depla et al. via pumping the vacuum chamber at different rates [22].

3.2. Target Voltage Control Point

The results shown in Figures 4 and 5 demonstrate that the measured target voltage hysteresis loops have typical characteristics of that for reactive magnetron sputtering deposition of compound films. The result also indicates that a small change in the oxygen flow would result in a switch from the metallic mode to the compound mode. In this work, the target voltage control approach is used to maintain the flow rate of the reactive gas at a desired flow rate. The aiming voltage of the sputtering target during the sputtering deposition of aluminum oxide is calculated according to the following formula:

$$V_A = V_C + (V_M - V_C) \times \eta \quad (1)$$

where V_A is the aiming target voltage, V_M and V_C the target voltage in the metallic mode and compound mode, respectively, and η the target voltage control point.

The deposition parameters of aluminum oxide films are shown in Table 1. It is obvious that under identical target power of 1.5 kW, the target voltage and the deposition rate of the obtained film increase with a rise in the control point. This is due to the fact that the rise of the control point drives sputtering to the metallic mode, which has higher target voltage and higher deposition rate.

Table 1. Deposition parameters of aluminum oxide films.

Sample No.	Control Point (η)	Target Power (W)	Target Voltage (V)	Deposition Time (min)	Film Thickness (nm)	Estimated Average Grain Size (nm)
1	25%	1500	412	60	506	84
2	30%		451		591	89
3	35%		488		724	87
4	40%		528		907	174

The surface morphology of the aluminum oxide films obtained under different voltage control points is shown in Figure 6. It is illustrated that the surface of the deposited films are made of fine grains with compact arrangements when the control point is between 25~35%. A similar result was obtained with a control point of 40%, but the grain sizes are relatively larger, which is probably due to higher deposition rate at 40%. For anti-corrosion purpose, the compactness property of the prepared film is of paramount importance, and large grain sizes would provide larger penetration channels for corrosive chemicals to reach the surface of the highly active metal substrate. Therefore, it is better to choose the control point between 25~35% for practical anti-corrosion applications.

The XRD results of the aluminum oxide films prepared under different voltage control points are shown in Figure 7. It is shown that these results are quite different from the XRD pattern of sputter deposited Al films, as shown in Figure 8. These results indicate that the prepared films are aluminum oxide with low level of crystallization. Therefore, the diffraction peaks are not evident and the obtained aluminum oxide films are mainly in the amorphous form.

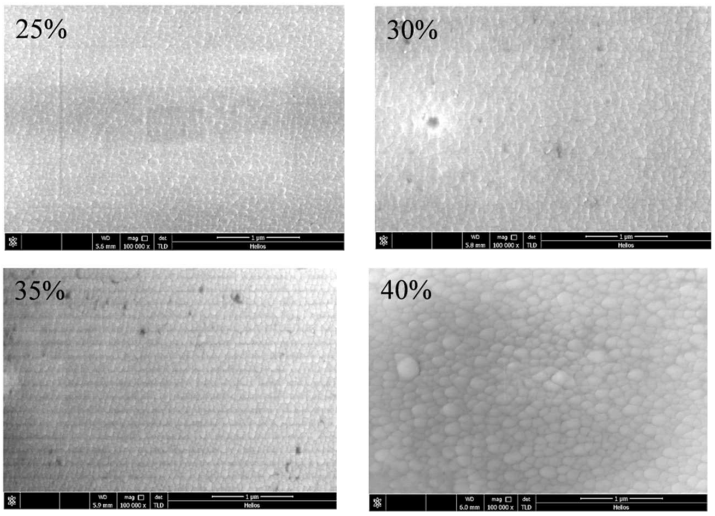

Figure 6. Surface morphologies of aluminum oxide film prepared at different target voltage control point. For all the images, the magnifications are 100,000, and the actual sizes are around 4.15 × 2.78 μm^2.

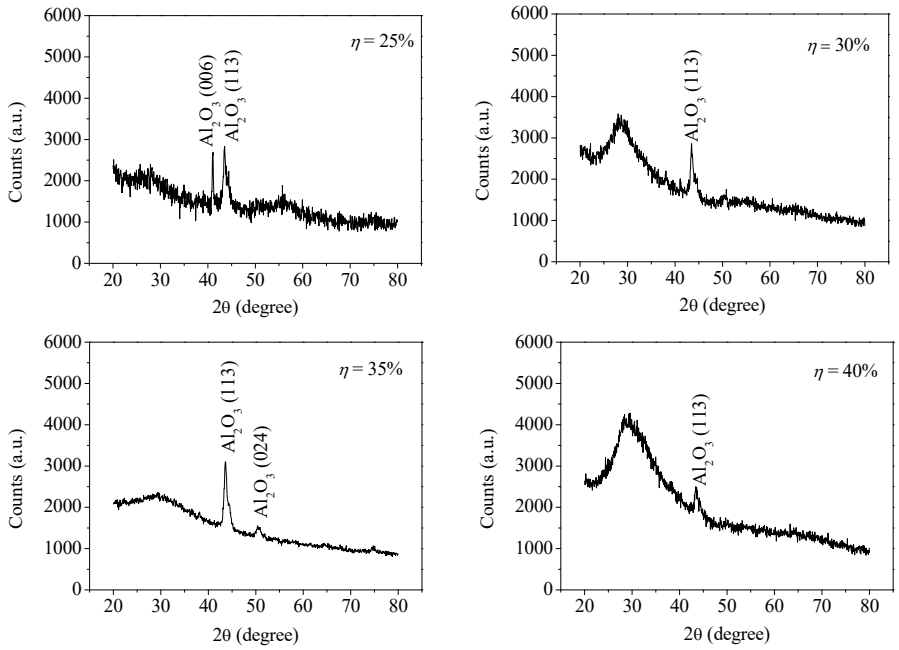

Figure 7. XRD patterns of aluminum oxide film prepared at different target voltage control points.

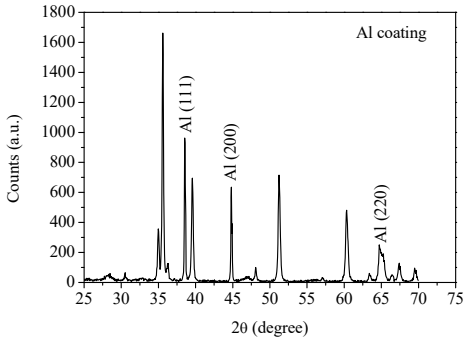

Figure 8. XRD pattern of sputter deposited Al film.

A typical EDS pattern of the prepared aluminum oxide films is shown in Figure 9. This data shows that traces of argon exist in the prepared oxide films. Two points contribute to this phenomenon: argon atoms are adsorbed by aluminum oxide particles, which has high melting point, in the reactive sputtering process, and therefore it is difficult for argon atoms to escape from these particles via the localized melting-reconstruction process; the reactive sputtering products are in the form of clusters of molecules and atoms with low diffusion mobility, and thereby it is unfavorable for the argon atoms to be repelled and de-adsorbed. Note that the signal of the Al element intensifies as the rise of the voltage control point. This is because that higher voltage control point leads to higher deposition rates; therefore, there are more Al atoms in the deposited oxide films.

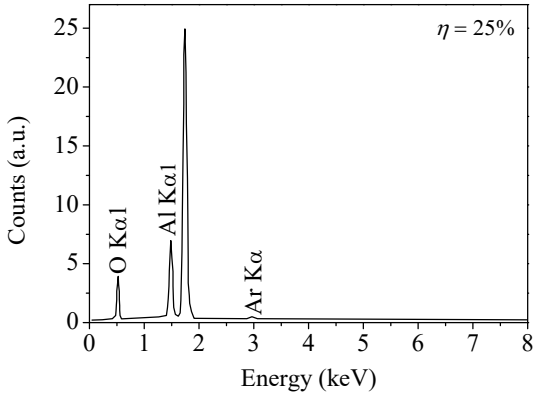

Figure 9. A typical EDS pattern of the deposited aluminum oxide film.

The atomic ratio of the prepared aluminum oxide films revealed by EDS quantitative analysis is shown in Figure 10. It is shown that all the films exhibit larger O:Al atomic ratio than the stoichiometric value of 3:2, which is due to the high oxygen flow rate under low target voltage control points. This implies that there are free O atoms, or that physically adsorbed O exists in the prepared oxide films. With a rise in the control point, the oxygen flow rate drops and the O:Al ratio becomes closer to stoichiometry.

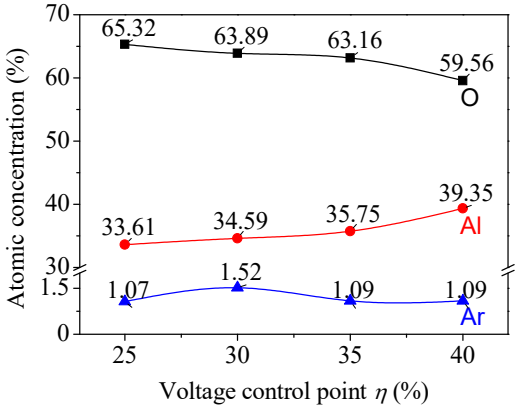

Figure 10. Atomic concentration of aluminum oxide films prepared under different control points revealed by EDS.

A typical AES pattern of the prepared aluminum oxide films is shown in Figure 11. It is apparent that the Al $L_{23}VV$, O KVV and Al $KL_{23}L_{23}$ Auger electron lines are identified clearly [24]. Based on these results, quantitative analyses have been performed and the atomic concentrations of O and Al are obtained and shown in Figure 12.

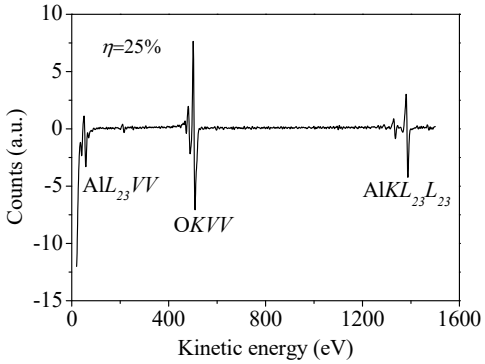

Figure 11. A typical AES pattern of the deposited aluminum oxide film.

The atomic concentration result of O and Al shown in Figure 12 is consistent with the result revealed by EDS measurements, as shown in Figure 10. Nonetheless, all the atomic ratios of O and Al are larger than the stoichiometric value, which again signifies that there are free O atoms in the bulk, or that are physically adsorbed into the surface of the aluminum oxide films.

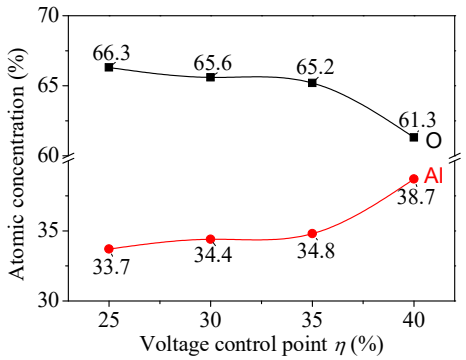

Figure 12. Atomic concentration of aluminum oxide films prepared under different control points revealed by AES.

4. Conclusions

The target voltage hysteresis phenomenon of medium frequency reactive sputtering deposition of aluminum oxide films has been investigated in this work. The obtained target voltage hysteresis loops, obtained under different argon partial pressure (0.2, 0.3, 0.4 and 0.5 Pa) and target power (1.0, 1.25 and 1.5 kW) conditions, are similar and have typical behaviors to those for reactive sputtering deposition of compound films.

The surface morphology, crystalline structure, and chemical composition of the aluminum oxide thin films prepared at different target voltage control points, have been investigated by SEM, XRD, EDS and AES. The results show that the prepared films are aluminum oxide, with low levels of crystallization and compact films, could be obtained with a target voltage control point between 25~35%. The atomic ratio of O and Al of the prepared oxide films are all slightly larger than stoichiometry, as revealed by EDS and AES measurements, which denotes that there are free O atoms exist in the bulk or physically adsorbed into the surface of the aluminum oxide films.

Based on the results of this work, optimal preparation conditions of aluminum oxide films could be developed. Similar process could be applied for the deposition of other compound thin films, such as oxides, nitrides and carbides. Further research on the corrosion resistance of aluminum/aluminum oxide multilayered coating is in progress.

Acknowledgments: This work is partially supported by the National Science Foundation of China (No. 61604138), and the Director's Funding of the Institute of Materials, China Academy of Engineering Physics (No. SJYB201509).

Author Contributions: Qingfu Wang and Liping Fang conceived and designed the experiments; Qinghe Liu and Lin Chen performed the sputtering experiments; Qinguo Wang contributed XRD; Xiandong Meng contributed SEM and EDS; Hong Xiao contributed AES; Qingfu Wang and Liping Fang analyzed the data and wrote the paper.

Conflicts of Interest: The authors declare no conflict of interest.

References

1. Xin, Y.; Huo, K.; Hu, T.; Tang, G.; Chu, P.K. Mechanical properties of Al_2O_3/Al bi-layer coated AZ91 magnesium alloy. *Thin Solid Films* **2009**, *517*, 5357–5360. [CrossRef]
2. Li, H.Q.; Wang, Q.M.; Gong, J.; Sun, C. Interfacial reactions and oxidation behavior of Al_2O_3 and Al_2O_3/Al coatings on an orthorhombic Ti_2ALNb alloy. *Appl. Surf. Sci.* **2011**, *257*, 4105–4112. [CrossRef]
3. Matikainen, V.; Niemi, K.; Koivuluoto, H.; Vuoristo, P. Abrasion, erosion and cavitation erosion wear properties of thermally sprayed alumina based coatings. *Coatings* **2014**, *4*, 18–36. [CrossRef]
4. Ali, R.; Saleem, M.; Pääkkönen, P.; Honkanen, S. Thermo-optical properties of thin-film TiO_2–Al_2O_3 bilayers fabricated by atomic layer deposition. *Nanomaterials* **2015**, *5*, 792–803. [CrossRef]
5. Pfeiffer, K.; Schulz, U.; Tünnermann, A.; Szeghalmi, A. Antireflection coatings for strongly curved glass lenses by atomic layer deposition. *Coatings* **2017**, *7*, 118. [CrossRef]
6. Lackner, J.; Waldhauser, W.; Major, L.; Kot, M. Tribology and micromechanics of chromium nitride based multilayer coatings on soft and hard substrates. *Coatings* **2014**, *4*, 121–138. [CrossRef]
7. Yin, A.; Yan, J.; Chen, L.; Zhu, S.; Long, Z.; Fang, L.; Liu, T. Experimental and numerical investigation of buckling and delamination of Ti/TiN coatings on depleted uranium under compression. *Appl. Surf. Sci.* **2017**, *422*, 997–1006.
8. Matthias, W.; Hoang Tung, D.; Hartmut, S.; Rainer, H. Aluminium atom density and temperature in a dc magnetron discharge determined by means of blue diode laser absorption spectroscopy. *J. Phys. D Appl. Phys.* **2005**, *38*, 2390–2395.
9. Kulczyk-Malecka, J.; Kelly, P.; West, G.; Clarke, G.; Ridealgh, J. Characterisation studies of the structure and properties of as-deposited and annealed pulsed magnetron sputtered titania coatings. *Coatings* **2013**, *3*, 166–176. [CrossRef]
10. Stefanov, B.; Österlund, L. Tuning the photocatalytic activity of anatase TiO_2 thin films by modifying the preferred grain orientation with reactive dc magnetron sputtering. *Coatings* **2014**, *4*, 587–601. [CrossRef]
11. Navabpour, P.; Cooke, K.; Sun, H. Photocatalytic properties of doped TiO_2 coatings deposited using reactive magnetron sputtering. *Coatings* **2017**, *7*, 10. [CrossRef]
12. Gao, W.; Li, Y.; Zhang, Y.; Yin, H. Exploration of growth window for phase-pure cubic boron nitride films prepared in a pure N_2 plasma. *Coatings* **2018**, *8*, 82. [CrossRef]
13. Safi, I. Recent aspects concerning dc reactive magnetron sputtering of thin films: A review. *Surf. Coat. Technol.* **2000**, *127*, 203–218. [CrossRef]
14. Bräuer, G.; Szyszka, B.; Vergöhl, M.; Bandorf, R. Magnetron sputtering—Milestones of 30 years. *Vacuum* **2010**, *84*, 1354–1359. [CrossRef]
15. Kouznetsov, V.; Macák, K.; Schneider, J.M.; Helmersson, U.; Petrov, I. A novel pulsed magnetron sputter technique utilizing very high target power densities. *Surf. Coat. Technol.* **1999**, *122*, 290–293. [CrossRef]
16. Anders, A. Discharge physics of high power impulse magnetron sputtering. *Surf. Coat. Technol.* **2011**, *205*, S1–S9. [CrossRef]
17. Stranak, V.; Herrendorf, A.-P.; Drache, S.; Cada, M.; Hubicka, Z.; Bogdanowicz, R.; Tichy, M.; Hippler, R. Plasma diagnostics of low pressure high power impulse magnetron sputtering assisted by electron cyclotron wave resonance plasma. *J. Appl. Phys.* **2012**, *112*, 093305. [CrossRef]
18. Sproul, W.D.; Christie, D.J.; Carter, D.C. Control of reactive sputtering processes. *Thin Solid Films* **2005**, *491*, 1–17. [CrossRef]
19. Depla, D.; Buyle, G.; Haemers, J.; De Gryse, R. Discharge voltage measurements during magnetron sputtering. *Surf. Coat. Technol.* **2006**, *200*, 4329–4338. [CrossRef]
20. Berg, S.; Nyberg, T. Fundamental understanding and modeling of reactive sputtering processes. *Thin Solid Films* **2005**, *476*, 215–230. [CrossRef]

21. Martin, P.M. *Handbook of Deposition Technologies for Films and Coatings: Science, Applications and Technology*; William Andrew: New York, NY, USA, 2009.
22. Depla, D.; Mahieu, S.; De Gryse, R. Depositing aluminium oxide: A case study of reactive magnetron sputtering. In *Reactive Sputter Deposition*; Depla, D., Mahieu, S., Eds.; Springer: Berlin/Heidelberg, Germany, 2008; pp. 153–197.
23. Smith, P.C.; Hu, B.; Ruzic, D.N. Low-energy ion-induced electron emission from gas-covered surfaces. *J. Vac. Sci. Technol. A Vac. Surf. Films* **1994**, *12*, 2692–2700. [CrossRef]
24. Briggs, D.; Seah, M. *Practical Surface Analysis: By Auger and X-ray Photoelectron Spectroscopy*; Wiley: Hoboken, NJ, USA, 2003.